The Institute of Space and Astronautical Science
Report No. 608, November 1983

Fine Pointing Control of the Solar UV Telescope on the Sounding Rocket S-520-5

By

Ichiro NAKATANI†, Tadanao SATO†, Toshizumi TANGE†, Shigeo HAMANA*, Tadashi HIRAYAMA*, Keizo NISHI*, and Kyo AKITA*

(October 17, 1983)

Summary: This report describes the performance of the attitude control system of a sounding rocket (S-520-5) and the fine pointing system incorporated in a solar ultraviolet telescope. The achieved pointing accuracy was within ±0.03 degree for the attitude control of the body, and within ±0.5 second of arc in the fine pointing for about half of the observing time.

Key words: attitude control, fine pointing, sounding rocket, solar UV telescope, gyro attitude reference.

1. INTRODUCTION

One of the missions of the Japanese sounding rocket S-520-5 was to obtain two dimensional pictures of a part of the sun using solar emission lines in 68.0–103.2 nm wavelength region. For this purpose it was necessary to achieve the telescope pointing accuracy of a few seconds of arc. Two kinds of pointing system were used: coarse pointing was performed by controlling the rocket [*1*] and fine pointing was carried out by a rapid tilting of one of the telescope mirrors. The former is designed to attain the pointing accuracy of the order of 0.1°, so that the latter can achieve the final arc second pointing. S-520-5 was successfully launched on September 6, 1982 and the required pointing accuracy was achieved.

2. ATTITUDE CONTROL OF THE ROCKET BODY

The required pointing accuracy of the rocket body is summarized as follows:

1) Angle error bias for pitch and yaw with respect to the sun: ±0.1°
2) Amplitude of limit cycle angle for pitch and yaw: 0.1°
3) Amplitude of limit cycle angle rate for pitch and yaw: $0.1°s^{-1}$
4) Amplitude of limit cycle angle for roll: 0.2°

These numerical values were specified considering the tolerance of the telescope optical

† Institute of Space and Astronautical Science.
* Tokyo Astronomical Observatory, University of Tokyo.

aberration and the time constant of the fine pointing system.

The alloted time for the acquisition of the above mentioned attitude is 118s during which about 21° attitude maneuver is necessary. In the initial control phase, two 5 m flexible antennas and several other sensors which could cause attitude disturbances were deployed. The effect of the 5 m flexible antennas was dominant and had been intensively investigated by means of simulation [2].

The attitude control system was designed to meet the above mentioned requirements, while new equipment and concept for control system had been introduced. The system is outlined below.

1) To realize a small limit cycle corresponding to high precision attitude, side jets with 100 g N_2 thruster were used. The engine configuration and firing logic are shown in Fig. 1.
2) As an attitude reference, gyros were used in the acquisition mode and a sun sensor was used after the acquisition of the sun was achieved.
3) As a gyro attitude reference, a spin-free-analytical platform system was used. This system consists of a spin stabilized platform and three RIG's (Rate Integrating Gryos) as shown in Fig. 2. Besides the RIG's, an RG (Rate Gyro) was used to

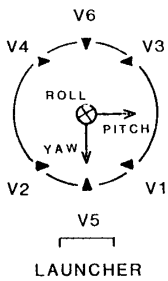

MODE IN WHICH EACH AXIS IS CONTROLLED INDEPENDENTLY

AXIS	ERROR COM	FIRED VALVES
ROLL	CW	V2,V3
	CCW	V1,V4
PITCH	UP	V5
	DOWN	V6
YAW	CW	V2,V4
	CCW	V1,V3

MODE IN WHICH YAW AND ROLL ARE CONTROLLED SIMULTANEOUSLY

		ROLL		
		CW	—	CCW
YAW	CW	V2	V2,V4	V4
	—	V2,V3	—	V1,V4
	CCW	V3	V1,V4	V1

Fig. 1. Engine configuration and its firing logic.

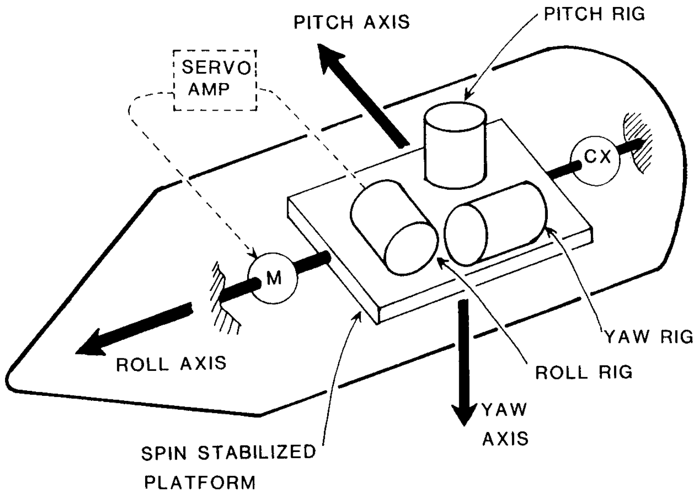

Fig. 2. Attitude measurement unit.

provide a roll rate damping signal. The detailed block diagram of the on-board attitude control hardware system is shown in Fig. 3.

4) A skew effect is inherent in a spin-free table system. A skew effect is the coupling of pitch and yaw to roll. This was compensated by applying the skew-compensation signal to the roll RIG torquer based on the result of on-board computer processing.

5) A 16-bit microprocessor was introduced to enhance the design flexibility and to achieve weight and size reduction. The required telemetry channel number was also reduced by multiplexing the signals by the processor. The clock frequency is 3MHz and the minimum instruction excuting time is 2.7 μs. The required memories are 4KW ROM and 512W RAM. The cycle time of the attitude detection and control is

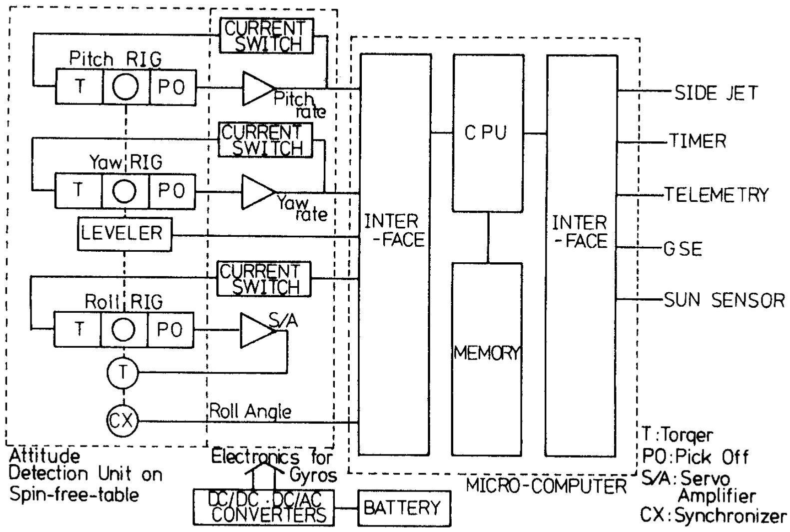

Fig. 3. Block diagram of attitude control system for S-520-5.

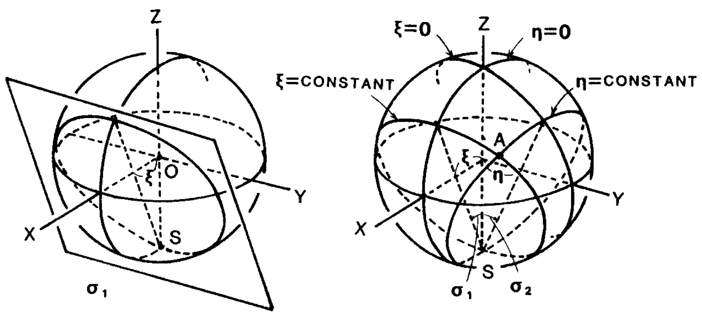

Fig. 4. Single pole coordinate system.

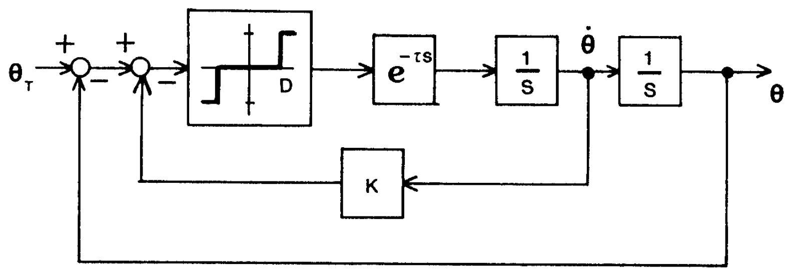

Fig. 5. Block diagram of attitude control system.

20 ms.

6) A single-pole coordinate ξ-η system was introduced to reduce the number of singular point. The ξ-η system is illustrated in Fig. 4.

7) The block diagram of attitude control system is shown in Fig. 5. An on-off control with dead band based on a linear combination of attitude and attitude rate signal was used for all 3-axes. In Fig. 5, τ is the time lag of side jet. Only rigid body dynamics is shown. Depending on the attitude and attitude rate, the following three modes were provided, and the three kinds of switching curves were used depending on the mode.

i) Mode 1: Before the coarse sun sensor acquires the sun, only gyros are used.

ii) Mode 2: The sun has been acquired, but the limit cycle is not achieved. The relation $|\theta|<1.25°s^{-1}$ holds. Under these conditions, the sun sensor is used.

iii) Mode 3: Mode 2 has been achieved and $|\theta|<0.5°$ holds. The limit cycle is supposed to have been achieved and the mode is never reversed.

The coarse sun sensor is composed of a 3 mm diameter pinhole and a two dimensional position sensitive detector which is separated by 80 mm from the pinhole. It covers a field view of $\pm 4°$ and the accuracy of angle determination is 0.03°, which is mainly limited by the resolution of the telemetry and to a lesser extent by the temperature dependence of LOG amplifiers.

1. Fine Pointing

The solar telescope-spectrograph (Fig. 6) was composed of a 100 mm aperture classical Cassegrain and a 500 mm-length stigmatic spectrograph whose diversed light is detected by a two dimensional microchannel plate (MCP) and a photomultiplier (PM). The ratio of focal distance to aperture of the telescope was 15. The description of the astronomical result together with appropriate instrumentation will be reported elese-

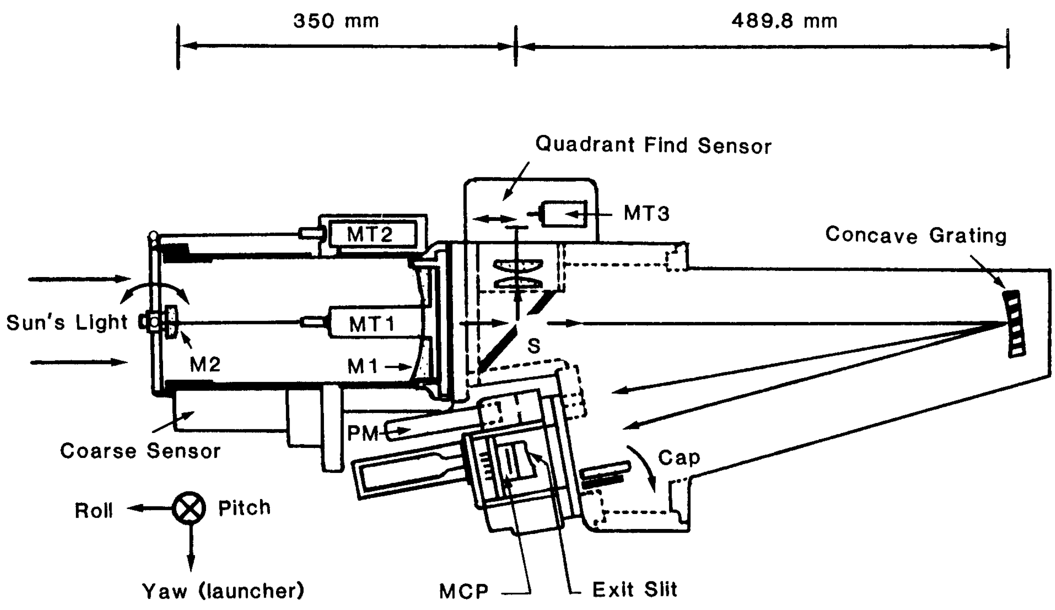

Fig. 6. Solar EUV telescope-spectrograph.

where.

The secondary mirror of the Cassegrain telescope (M_2) is supported by a gimbal structure. And this is connected to two motors (MT_1 and MT_2) through rods so that fine tilting is possible in two directions (pitch and yaw). However there is no fine pointing on the roll axis. The sun's light is reflected by 45° just on the spectrograph mirror-slit (S) and the solar image on the slit is refocused by transfer lenses onto a quardrant position detector (QD320, Centronic Co.). This detector measures the center position of the solar image and the error signal of the center position is fed back to the two motors. The voltage is applied to these motors in proportion to the error signal, namely difference signals in pitch and yaw. A third motor, MT_3, is used to drive the position sensor unit in a direction parallel to the roll axis and hence to provide a scanning capability over the solar image (raster scan mode).

The block diagram of the fine pointing is shown in Fig. 7. And the open loop transfer function of the system is given by

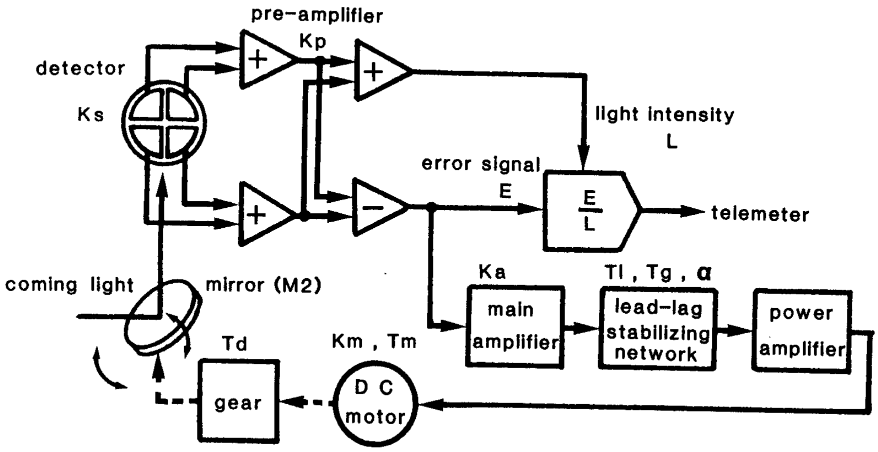

Fig. 7. Block diagram of the fine pointing system. Detector connection is only e.g. for yaw.

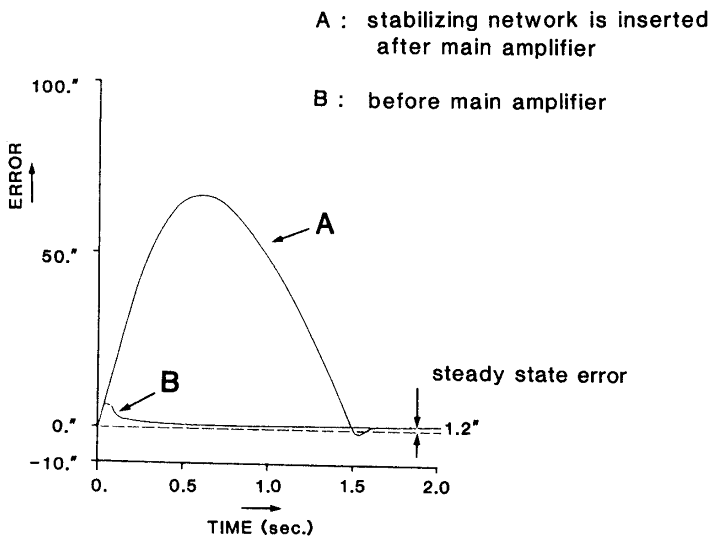

Fig. 8. Simulated transient response to a ramp-function input (0.1° s^{-1}).

Table 1. System characteristics of the fine pointing

Sensitivity of the detector	K_s	9.4 mV arcsec^{-1}
Voltage gain of pre-amplifiers	K_p	10
Voltage gain of main amplifier	K_a	73.5
Time constant of the motors (MT_1 and MT_2)	T_m	11 ms
Transfer constant of the motor-gear block	K_m	45 arcsec s^{-1} V^{-1}
Transfer delay time of the motor-gear block	T_d	about 20 ms
Overall gain constant	$K_s \cdot K_p \cdot K_a \cdot K_m$	310 s^{-1}
Time constant of phase lead network	T_1	27 ms
Time constant of phase lag network	T_g	0.2 s (yaw) 0.3 s (pitch)
Attenuation constant of the network	α	0.25
Hunting frequency (unstabilized)		6 Hz
Steady state error for 0.1° s^{-1} ramp-function input		1.2 arcsec
Maximum mirror speed (in terms of deflection rate of the sun's light)		0.15° s^{-1}
Saturation voltage of the main amplifier		12 V

$$G(s)=\frac{K_sK_pK_aK_m(1+sT_1)(1+sT_g)}{s(1+sT_m)(1+s\alpha T_1)(1+sT_g/\alpha)}\exp(-sT_d).$$

Here saturation effort is neglected. Various constants appearing in Fig. 8 and in the above equation are summarized in Table 1. The DC servo-motors (MT_1 and MT_2, ESCAP 23D21-216E) have been chosen by considering a small time constant (11 ms) and a fairly wide dynamic range (starting voltage/maximum voltage=0.3 V/12V). Simulated transient responses to a ramp-function input are shown in Fig. 8. Laboratory experiments for the same 0.1°s^{-1} input showed a similar steady state error of 1.2″ with fluctuation of ±1″ and an overshoot error of 60″–70″ with duration of 1.0–1.3s, and they are consistent with the simulation A; in the actual flight a stabilizing network was inserted *after* the main amplifier as with the case A. Since the saturation is expected in the actual circuit, we should have placed the stabilizing network *before* the main amplifier (case B in Fig. 8). In pre-flight experiments large amplitude oscillations of ±15″ with a period of 3s and with a duration of few cycles occurred as the pitch error when the third motor, MT_3, changed direction of the movement. To avoid this effect a slightly larger time constant was adopted for pitch.

4. Control Sequence

Since three hours before the launch of the rocket, on-board attitude measurement unit and electronics for body pointing had been checked out by means of GSE (Ground Support Equipment) which consists of operation console and a mini-computer. The set angles of a launcher were decided 75 minutes before the launch and the gyro set angle was calculated and set automatically by GSE based on the launcher angle data. The rocket was given 2 rps spin aerodynamically. The spin was reduced to 0.3 rps at 45s after the launch by releasing a yo-yo despinner and it was further reduced by the side jets. The payload section was separated from the burnt out engine at 60s and the attitude control of the body was started at 62s.

At 150s, the initial target attitude of the rocket was acquired and the fine pointing of the telescope was started. At 150s after the launch (UT $02^h00^m00^s$), the observation was started without actuating the raster scan motor (MT_3), while from 180s to 420s it was rotated back and forth to perform raster scanning.

5. Flight Result

For the body control equipment, 24 telemetry items are allocated from which the attitude history of the rocket was calculated on an off-line basis. Examples of the results are shown in Fig's 9 through 11. In Fig. 9, roll angle history is shown. Roll angle is expressed as an angle between $-180°$ and $+180°$. The locus of the nose direction of the rocket body is shown in Fig. 10. At about 80s, the initial attitude was acquired which was maintained till 430s. In the initial 3.5s period, a sharp nose dive can be observed

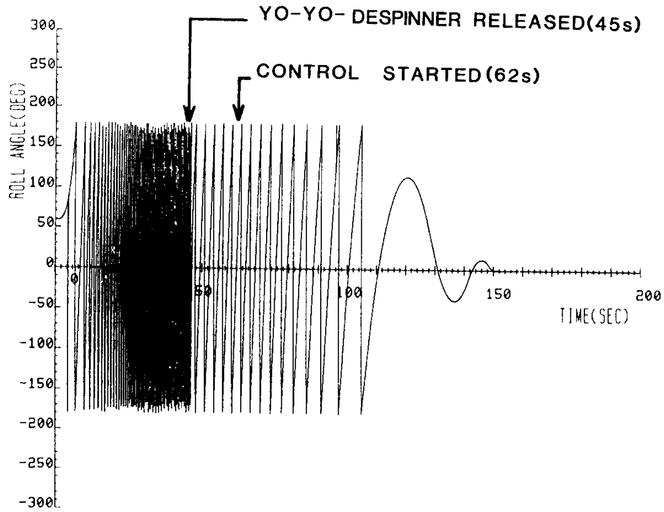

Fig. 9. Roll angle vs. time.

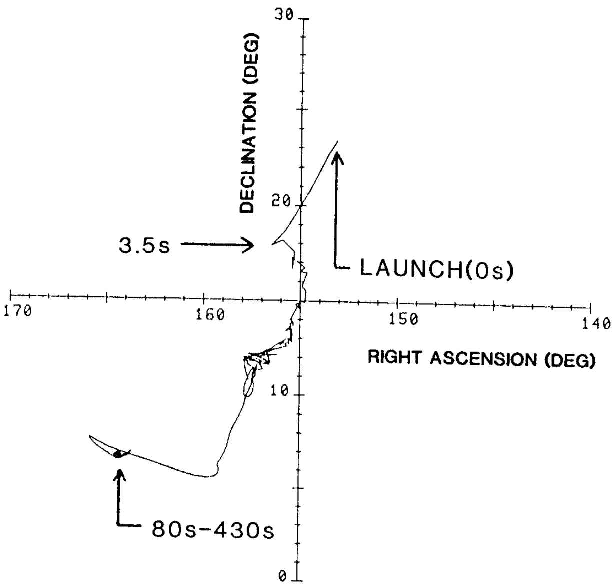

Fig. 10. Locus of nose direction determined by gyro.

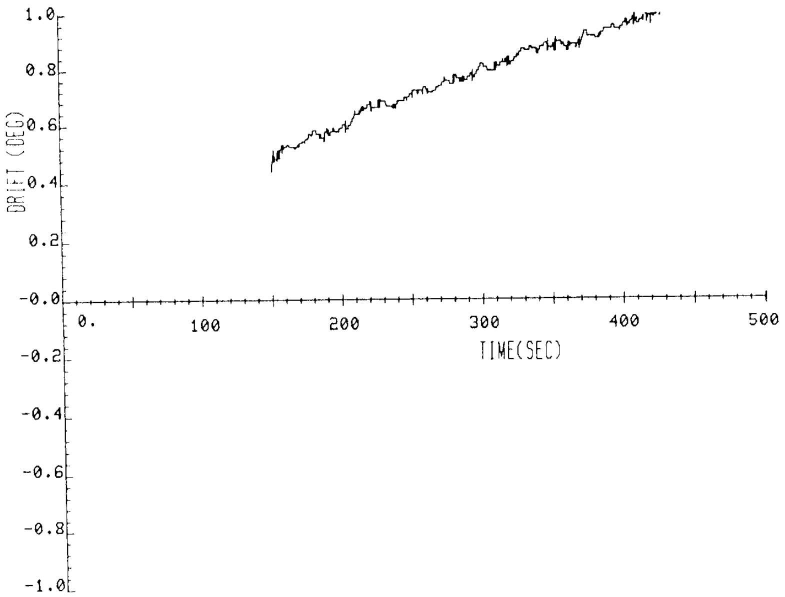

Fig. 11. Gyro drift in right ascension direction vs. time.

followed by precession, nutation and wobbling. Gyro drift calculated by the sun sensor data is shown in Fig. 11.

In Fig. 12 the time history of the pitch and yaw error angles for the fine pointing system is shown together with the raster angle. The on-off history of the jet valves and the attitude history of the rocket body are also shown. From Fig. 12, we can say that the yaw error remained within two arc sec for 97% of the observation time, while the pitch error remained within two arc sec only 54%. For most of this 2″ pointing period, the telemetry data show ±0.5″ pointing accuracy was achieved which is the limit of the 8 bit telemetry. Hence we may conclude that for about half of the observation time, the fine pointing remained within ±0.5″ accuracy.

The profiles of large amplitude oscillations in the pitch error (4s period and typically 25″ amplitude) are quite similar to those met in the pre-flight experiment when raster direction was changed. However in the actual flight the large oscillations did not occur at the change of raster scans. Nor were they related to the timing of the on-off of the side jets as shown in Fig. 12. Although real cause is not clear, the large oscillations might be related to the saturation effect mentioned above.

It was however possible to construct a single solar image from two raster scans by using only those portions where less than 2″ fine pointing was attained as can be judged from Fig. 12. Examples of the solar image in the light of an emission line of doubly ionized carbon at 97.7 nm, and hydrogen Lyman continuum emission at 88.0 nm with a pass band of 1.6 nm are shown in Fig. 13. Eight pictures of these kinds in total (MCP) have been successfully obtained together with one dimensional scan (PMT) at 165.0 nm. Here the solar diameter is 1907″. The spatial resolution of the actual pictures in Fig. 13 is approximately 10″×10″ in spite of an overall pointing accuracy less than 2″, and in spite of the fact that the effective pixel size of the detector MCP was as small as 5″. This is not only because photon numbers received from the most of the quiet region of the sun were not large, but also because the focusing was not complete. We were extremely

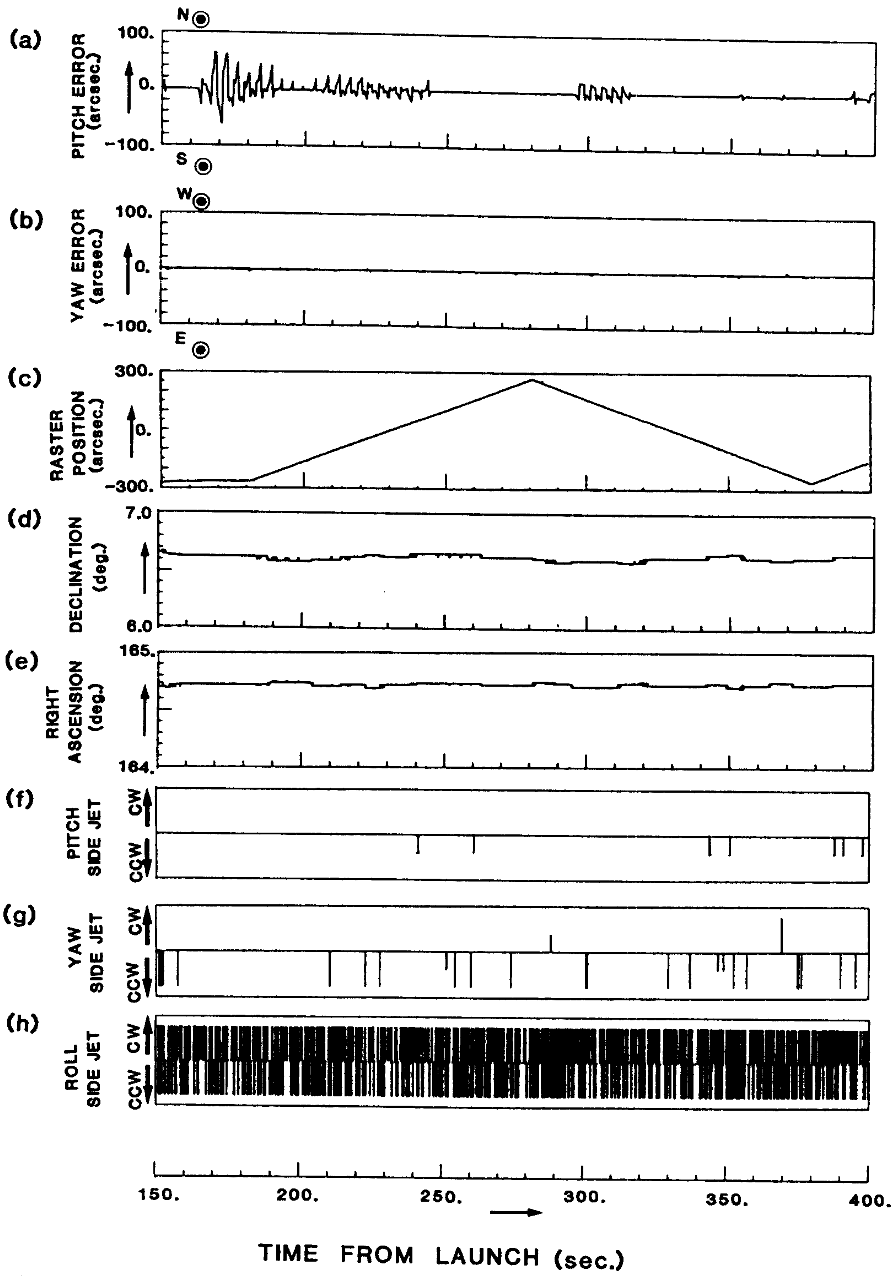

Fig. 12. The result of the fine pointing during the flight. In the bottom are shown timings of side jets. (see Fig. 1 for the definition of V's).

fortunate to have encountered the flaring of a part of the sun (a solar flare class of 1B and C3, September 6, 1982, UT $01^h50^m-02^h20^m$).

6. Conclusions

The requirements for the attitude control of the rocket body were completely met and it was demonstrated that the above mentioned coarse control system can be a standard type for S-520 series rockets. The expected attitude disturbance by flexible antennas was not seen, implying a very small deflection of the antennas in the initial deployment. The

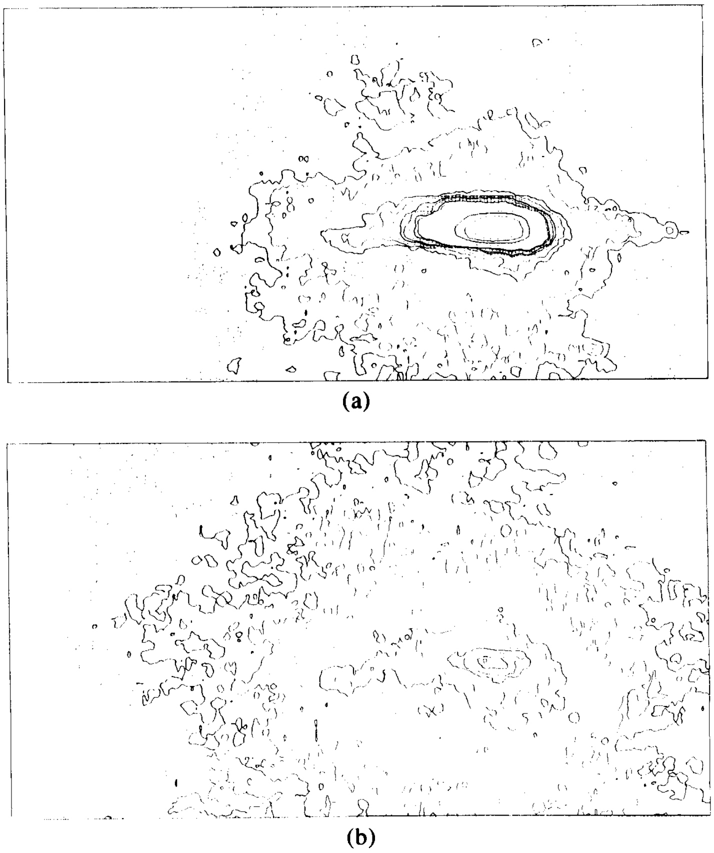

Fig. 13. Example of a part of the solar image obtained at 97.7 nm of doubly ionized carbon emission line (a), and at 88.0 nm of hydrogen Lyman continuum (b). Picture size is 1040×550 seconds of arc. Top is solar north, west is on the right. The flare is near the center at the highest portion in these iso-intensity maps.

body attitude after the limit cycle had been acquired was stable with jet on-off less frequent than expected. The reason is under investigation. Gyro drift was larger than expected. The problem is assumed to be with on-board data processing software system which is now being investigated.

The fine pointing accuracy of less than two seconds of arc was achieved and the satisfactory solar images in the ultraviolet light were obtained. As to the absolute attitude accuracy of the fine pointing, we can only say that it was less than one to two arc minutes since we did not specify precisely, prior to the flight, where we were going to observe. This is because we had planned to cover a rather large area on the sun (17′×9′).

The body pointing was conducted by the ISAS group, while the group from Tokyo Astronomical Observatory was in charge of the fine pointing system together with the coarse sun sensor for the body pointing.

We acknowledge our indebtness to Profs. K. Hirao, R. Akiba, and H. Matsuo, and to the staffs of Tokyo Astronomical Observatory.

REFEREMCES

[*1*] Nakatani, I., Inst. of Space and Astronautical Science Report, S.P. **1**, 87, 1983.
[2] Nakatani, I., *et al.*, "Attitude Control System of the Sounding Rocket S-520-5", Proceedings of the International Symposium on Space and Science, 1982, Tokyo.